

Nonparametric Causal Feature Selection for Spatiotemporal Risk Mapping of Malaria Incidence in Madagascar

Rohan Arambepola

Oxford Big Data Institute, Nuffield Department of Medicine, University of Oxford

E-mail: rohan.arambepola@stx.ox.ac.uk

Peter Gething

*Oxford Big Data Institute, Nuffield Department of Medicine, University of Oxford;
Telethon Kids Institute, Perth Children's Hospital, Perth, Australia;
and Curtin University, Perth, Australia*

Ewan Cameron

Oxford Big Data Institute, Nuffield Department of Medicine, University of Oxford

Summary. Modern disease mapping uses high resolution environmental and socioeconomic data as covariates, or 'features', within a geostatistical framework to improve predictions of disease risk. Feature selection is an important step in building these models, helping to reduce overfitting and computational complexity, and to improve model interpretability. Selecting features that have a causal relationship with the response variable (not just an association) could potentially improve predictions and generalisability, but identifying these causal features from non-interventional, spatiotemporal data is a challenging problem. Here we apply a causal inference algorithm—the PC algorithm with spatiotemporal prewhitening and nonparametric independence tests—to explore the performance of causal feature selection for predicting malaria incidence in Madagascar. This case study reveals a clear advantage for the causal feature selection approach with respect to the out-of-sample predictive accuracy of forward temporal forecasting, but not for spatiotemporal interpolation, in comparison with no feature selection and LASSO feature selection.

1. Introduction

Spatial mapping of malaria risk is an important public health tool, facilitating the efficient allocation of limited resources and the precision targeting of interventions (Elliot et al., 2000; Lawson et al., 1999; Drake et al., 2017). While maps produced to-date have typically focussed on annual summaries of risk (e.g. Bhatt et al. 2015), there is increasing interest in making predictions at higher temporal resolutions (Colborn et al., 2018; Haddawy et al., 2018; Nguyen et al., 2019). Monthly or weekly risk maps have the potential to improve the timing of control strategies which rely on knowledge of seasonal trends in transmission, such as indoor residual spraying and seasonal chemoprevention (Griffin et al., 2016; Landier et al., 2018), and to aid in real-time prediction of outbreaks for malaria early warning systems (Girond et al., 2017; Minakawa et al., 2018; Pan et al., 2018; Tompkins et al., 2018).

Modern disease mapping methods combine disease surveillance data with covariate information (including satellite image products, weather station-derived inputs and travel

time surfaces (Weiss et al., 2018)) reflecting both the natural and built environments to produce smooth, high resolution risk maps within a probabilistic framework (Bhatt et al., 2013, 2015; Gething et al., 2016; Kang et al., 2018). Due to the wealth of products available as potential covariates some form of feature selection is important to avoid overfitting and improve predictive performance. Feature selection is particularly challenging when mapping at higher temporal resolutions, as the possibility of including each product at a number of time lags can result in a large number of often highly correlated features to choose from. Substantial variations observed in the seasonal pattern of malaria transmission, even in nearby locations (Singh et al., 2000) or year-to-year in the same locations (Reiner et al., 2015), suggest a complex system of interactions between environmental variables, socioeconomic factors and disease risk. As model flexibility is increased to capture these dynamics, the potential for overfitting to chance associations between features and response data is expected to grow, motivating interest in effective feature selection procedures.

Classical feature selection procedures aim to maximise model fit or predictive performance with respect to the observed data—as measured, for example, through cross-validation-based metrics or information criteria—while penalising the size of the feature set; typically retaining features with large associations with the response variable or those that are strong predictors within the model framework (Guyon and Elisseeff, 2003; Liu and Motoda, 2007). In contrast, causal feature selection methods (Guyon et al., 2007) aim to select features that have a direct causal relationship to the response variable even if the association is comparatively weak, excluding features that are only associated with the response variable due to common causes or through mediating variables.

Causal feature selection has been applied to several real-world datasets across diverse application areas including photo-voltaic cell engineering, financial time series forecasting, and medical prognosis, with mixed results: improvements in predictive accuracy over non-causal feature selection approaches in some cases (Hmamouche et al., 2017; Sun et al., 2015; Zhang et al., 2014), but not others (Cawley, 2008). Many causal inference algorithms depend on conditional and unconditional independence tests (Spirtes et al., 2000), but the most commonly-used independence tests require strong assumptions (such as joint normality) which may not hold true when using spatiotemporal environmental and epidemiological data. Here we apply spatiotemporal prewhitening (Flaxman et al., 2016) and independence tests based on the theory of kernel embeddings (Muandet et al., 2017) within the PC algorithm for graph discovery (Spirtes and Meek, 1995; Spirtes et al., 2000) to perform nonparametric causal feature selection in an explicit spatiotemporal setting. These features are used in a Bayesian hierarchical model for predicting malaria incidence in Madagascar, and the results compared to those from the same model fit without feature selection and with LASSO feature selection (a common non-causal method; Tibshirani 1996; Park and Casella 2008).

1.1. Malaria risk mapping

Visualisation of raw epidemiological and/or entomological data (e.g. health facility case numbers or prevalence of malaria from health surveys) is an important first step in characterising spatiotemporal patterns in malaria risk for a given area, but these data may suffer biases and incompleteness due to low treatment-seeking rates and incomplete

record keeping (amongst other factors). Relying on raw data is also problematic in pre-elimination settings, where the low transmission rates lead to a very noisy sampling distribution for standard malaria metrics. Modern disease mapping uses a formal statistical framework combining random field models with high resolution covariate data to achieve spatial smoothing and interpolation of raw data (Ribeiro Jr et al., 2001; Diggle et al., 2013; Bhatt et al., 2013; Shearer et al., 2016; Gething et al., 2011; Bhatt et al., 2015). These maps are used for allocation of resources, both on a global and local scale, and for precision targeting of interventions (World Health Organization, 2019).

1.2. Malaria in Madagascar

Malaria is a major public health problem in Madagascar with an estimated 2.16 million cases occurring in 2018 (World Health Organization, 2019). After a large reduction between 2000 and 2010, reported case numbers have been steadily increasing. Although perhaps partly due to improvements in access to rapid diagnostic capabilities, these data are nevertheless believed to reflect in some part a genuine increase of malaria transmission in the country (Howes et al., 2016). This increase in reported confirmed cases is corroborated by community-based infection prevalence data from community health surveys (Kang et al., 2018). In the medium and high transmission zones of Madagascar the clinical incidence rate typically follows a seasonal pattern peaking in April-May, although an earlier February peak has been observed in some places. Annual trends are less consistent in low transmission areas where instead temporal variation displays an outbreak dynamic (Howes et al., 2016; Randrianasolo et al., 2010), with unusual climatic events and changes in intervention coverage as key risk factors (Kesteman et al., 2016). The dominant species of malaria parasite on the island is *Plasmodium falciparum*, although *Plasmodium vivax* is also endemic in some areas (Howes et al., 2018; Kesteman et al., 2014).

1.3. Causal feature selection

It is well known that an association between two variables X and Y in observational data does not necessarily imply a causal effect (“correlation does not equal causation”) due to the possible existence of confounding variables (that is, other variables which have a causal effect on both X and Y). Part or all of the observed relationship between X and Y could be due to these common causes. The best method for discovering the causal effect of a variable X on variable Y is through a randomised control trial (RCT), as the randomisation removes any causes of X and therefore removes all confounding variables. However, there are many situations in which RCTs are not possible (for example, when investigating the causal effect of environmental variables) and instead only observational data is available. Causal inference methods (e.g. Rubin 2005; Pearl 2009) aim to discover causal relationships and effects from such ‘opportunistic’ or ‘retrospective’ data.

While understanding causality is not necessary for effective prediction in a purely observational setting, selecting features based on causal relationships might be desirable for a number of reasons. Causal feature selection could produce much smaller feature sets in situations where the response variable is correlated with many features but directly caused by relatively few (Guyon et al., 2007). Smaller feature sets may reduce overfit-

ting and allow for the use of more flexible models. The use of causal feature selection could also improve the interpretability of predictive models, where it is often hoped that structure of the fitted model is a reflection of the fundamental mechanistic properties of the system (Guyon et al., 2007). Models built on causal feature sets may also be more robust to common problems such as concept drift and covariate shift (Schölkopf et al., 2012) and therefore make more useful predictions further forward in time or in previously unobserved locations. Finally, nonparametric causal selection can be thought of as a form of model-free feature selection and therefore may be used in combination with ‘over-parameterised’, machine learning-style models for which classical feature selection methods may be unsuitable.

2. Methods

2.1. Data

Monthly malaria case data were available from the Madagascar National Malaria Control Program (NMCP) between January 2013 and December 2016. These data represent individuals who seek care at a health facility where a diagnosis of malaria is made and where that case is then recorded and entered into the national surveillance system. Such data are termed ‘passive’ case detection and rarely capture all malaria incidence in the community, as some cases do not seek care or do so from informal or private providers. These data do not differentiate by the species of malaria parasite causing the infection. Data were available 3342 health facilities in Madagascar, of which 2131 were geolocated and had catchment population estimates (NMCP, pers comm). Of these, complete case data was available at 573 health facilities (available for each month from 2013-2016) and a further 627 health facilities had mostly complete data (missing fewer than 3 months). Subsets of the health facilities with complete data were used as training data for the models while the remaining facilities with complete data and those with mostly complete data were used as testing locations. The locations of these health facilities are shown in Fig. 1. Models were fit with one year of case data at training locations and monthly incidence rate predictions were then made for the following two years at both training and testing locations.

The covariate products gathered to assist with probabilistic interpolation and forecasting of the case data are summarised in Table 1. Covariates used were dynamic and were included at 0, 1, 2, and 3 month time lags to allow covariate selection to identify the optimal variables and time lags to include in the final model. All of these variables are commonly used in malaria risk mapping and have putative causal connections to malaria incidence, however the relative importance of these factors in any given location and the exact time scales on which they act is not necessarily known.

2.2. Hierarchical Bayesian Model

The malaria case numbers reported by health facilities, $i = 1, \dots, N$, in months, $t = 1, \dots, M$, are modelled here as realizations of Poisson random variables with means, $\mu_{it} = \lambda_{it} \times p_i$, formed as the product of the local case rate, λ_{it} , with the size of the catchment population of the corresponding health facility, p_i . The latter being supplied as an additional datum by the Madagascar NMCP, which we treat for simplicity as

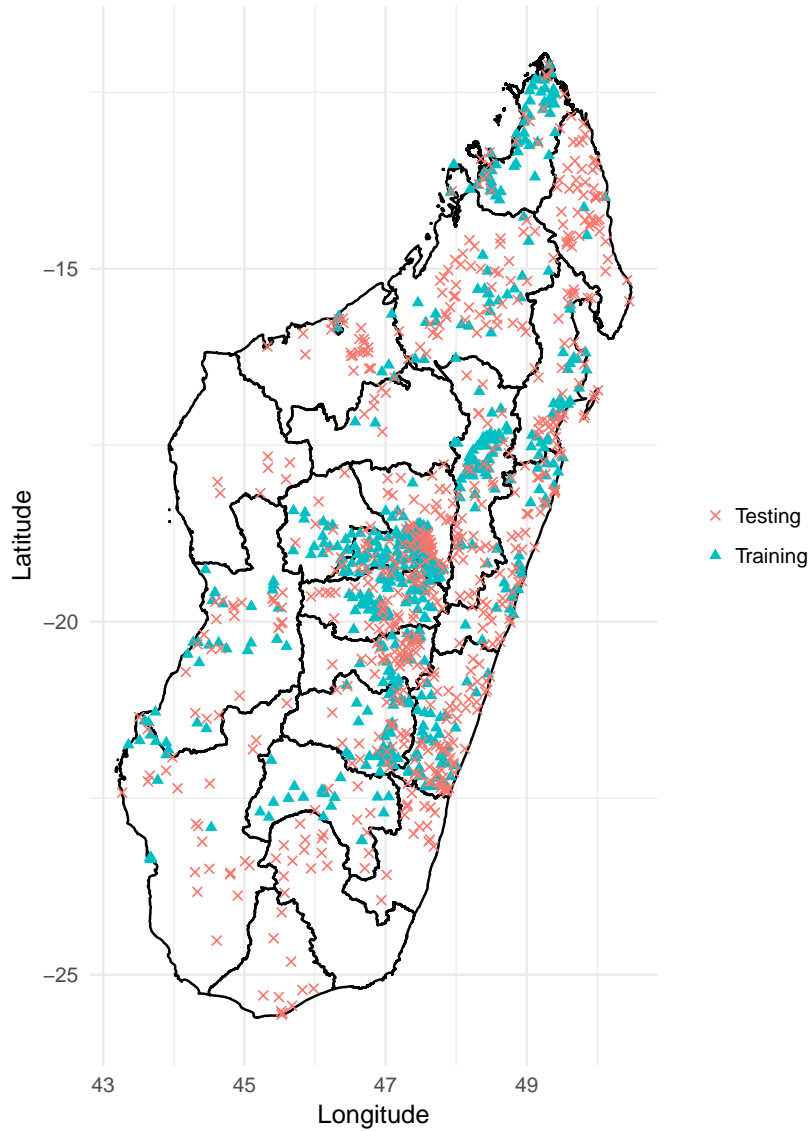


Fig. 1. Locations of health facilities in Madagascar for which malaria case data were available at monthly cadence between 2013 and 2016, with membership of either the training or testing libraries of this study distinguished by plotting symbol.

if precisely known. Following the conventions of model-based geostatistics the local incidence rate is modelled as the additive combination of a spatially autocorrelated noise term, ϵ_i , drawn from a Gaussian Process (GP) with Matérn kernel and some function, $f(\cdot)$, of the given covariates, X_{it} , i.e.,

$$\log \lambda_{it} = f(X_{it}) + \epsilon_i. \quad (1)$$

Table 1. List of covariates

Covariate	Description	Source
CHIRPS	Climate Hazards Group Infrared Precipitation with Station Data	CHIRPS (Funk et al., 2014)
LST day	Daytime land surface temperature	MODIS derivative (NASA Earth Observations, 2017)
LST night	Night-time land surface temperature	MODIS derivative (NASA Earth Observations, 2017)
TCB	Tasselled cap brightness; measure of land reflectance	MODIS derivative (NASA Earth Data, 2017a)
EVI	Enhanced vegetation index	MODIS derivative (NASA Earth Data, 2017b)
TSI Pf	Temperature suitability index for <i>P. falciparum</i>	MAP (Weiss et al., 2014)
TSI Pv	Temperature suitability index for <i>P. vivax</i>	MAP (Gething et al., 2011)

Two alternative forms of $f(\cdot)$ are considered in this study. The first is a linear combination of covariates,

$$f(X_{it}) = \beta_0 + \boldsymbol{\beta}^T X_{it} \quad (2)$$

where $\beta_0 \in \mathbb{R}$ and $\boldsymbol{\beta} \in \mathbb{R}^K$ are model parameters (to be assigned suitable priors and learned in the inference stage). The second form is a sum of univariate GPs in each covariate,

$$f(X_{it}) = \beta_0 + \sum_{l=1}^K \text{GP}_l(X_{it}). \quad (3)$$

where kernel of each GP, $k_l(\cdot, \cdot)$, takes the squared exponential (or ‘radial basis function’) form,

$$k_l(x, y) = \sigma^2 \exp\left(-\frac{(x - y)^2}{2\lambda_l^2}\right). \quad (4)$$

In this case the shared output scale, σ , and individual input scale-lengths, $\lambda_1, \dots, \lambda_K$, are model parameters. Compared to the linear version, the additive GP version allows for a more flexible representation of the relationship between each covariate and the log-incidence rate, though still being of limited complexity in ignoring interactions. A normal prior was placed on $\log \lambda_l$ with mean scaling with the number of covariates such that the prior correlation between points is roughly the same across feature sets of difference sizes.

In each experiment, for each version of $f(\cdot)$, a year of case data at locations within the training library was used for feature selection (if any) and to fit the model. Monthly predictions of incidence rate were then made for the following two years at both training and testing locations. This procedure was repeated for multiple training sets of different sizes. The performance of the linear model was compared across causal feature selection, LASSO selection and no selection, while the GP model was compared across causal selection and no feature selection.

When studying data gathered through routine health surveillance systems it can often be difficult to accurately estimate the absolute normalisation of incidence rates due

to uncertainties regarding treatment seeking propensities and numerous other factors, even outside of a low resource setting (e.g. Ali et al. 2015). For this reason, we focus in the subsequent analysis on a correlation-based performance metric designed to probe the ability of these models to achieve relative risk stratification rather than one probing absolute incidence rate estimation (e.g. root mean squared error; RMSE). In particular, when examining the performance of spatiotemporal interpolation we calculate the average correlation between predicted and observed values over all months and locations tested, and when assessing forward temporal forecasting we calculate the average of the correlations between predicted and observed time series at each location tested (which we term ‘mean local correlation’). For completeness, we also present RMSE diagnostics in the supporting materials.

Both models were implemented in R (R Core Team, 2018). The linear model was fit using the Template Model Builder package (Kristensen et al., 2016) and the GP model was fit using the Reticulate package (Ushey et al., 2019) and Pytorch (Paszke et al., 2019).

2.3. Causal feature selection

2.3.1. PC Algorithm

Causal inference algorithms aim to infer causal relationships between variables, as represented by directed acyclic graphs (DAGs), from purely observational data or a mixture of observational and interventional data. These algorithms are typically either constraint-based (Spirtes et al. 2000; such as the PC algorithm: Kalisch and Bühlmann 2007; Spirtes and Meek 1995), score-based (such as the Greedy Equivalence search algorithm: Chickering 2002), or a combination of the two (Nandy et al., 2018; Tsamardinos et al., 2006). We implemented the PC algorithm, which uses conditional independence testing, to infer causal relationships from observational data only.

In the DAG representation of causality an edge, $X \rightarrow Y$, implies that the variable, X , is a cause of variable, Y . Given a DAG describing a system of random variables, the *Markov property* states that a variable, X , is independent of any non-descendants given its parents and therefore any DAG implies a series of conditional independence relations. For example, the graph in Fig. 2 implies that X and Y are independent given Z , and in fact this is the only independence relation given by the Markov property in this graph. Conversely, a distribution is said to be *faithful* to a DAG if the only independence or conditional independence relations present in the distribution are those implied by the Markov property. For example, any distribution in which $X \perp\!\!\!\perp Y$, $X \perp\!\!\!\perp Z$ or $Y \perp\!\!\!\perp Z$ would not be faithful to the DAG in Fig. 2.

By the Markov property and assuming faithfulness, the DAG describing a set of random variables is constrained by the conditional independence relations between these variables. Given joint observations of the variables, these constraints can be discovered using conditional independence tests. The PC algorithm starts with a complete undirected graph, equivalent to no independence relations between variables, and uses conditional independence tests to recursively remove edges, returning as output an equivalence class of DAGs that are compatible with the observed independence relations. This algorithm runs in polynomial time when the true DAG is sparse (Kalisch and Bühlmann, 2007) and is consistent given consistent independence tests (Spirtes et al., 2000).

We applied the PC algorithm in two steps, first estimating the causal structure between the environmental variables at various time lags and subsequently estimating the relationships between the environmental variables and malaria incidence. This meant the observations used when discovering causal structure between environmental variables were not limited to locations of observed health facilities and therefore this structure could be learned with more confidence using data points from a greater number of locations. To perform this first step we implemented a standard order-independent variation of the PC algorithm (Colombo and Maathuis, 2014). To perform the second step, we began with the causal structure inferred between environmental variables and added a node representing malaria incidence (with no time lag) which was connected to all other nodes. We then applied a modified version of the PC algorithm to this graph in which only pre-specified edges were tested and potentially removed, in our case the edges to be tested were any edges with malaria incidence as a vertex. At each step the input graph did not include edges that would imply causation backwards in time (e.g. rainfall with a time lag of one month causing temperature with a time lag of two months) or malaria having a causal effect on the environment (i.e. any directed edge from incidence to an environmental variable).

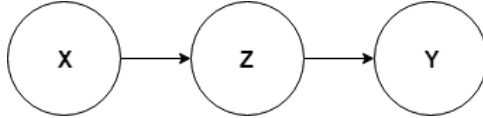


Fig. 2. An example of a directed acyclic graph describing the causal relationships between three random variables.

2.3.2. Nonparametric independence testing

The PC algorithm depends on the existence of appropriate independence and conditional independence tests, however many common parametric tests make strong assumptions about the underlying joint distribution of variables. For example, the χ^2 test for partial correlations assumes the variables are jointly normal. These assumptions may not hold in practice as variables in disease mapping are often a mixture of types—discrete (e.g. case numbers) and continuous (e.g. rainfall, temperature)—and are infrequently normally distributed (and rarely jointly so). We therefore implemented nonparametric independence and conditional independence tests based on the theory of kernel mean embeddings (Muandet et al., 2017), which place fewer assumptions on the underlying joint distribution of the variables.

Given an appropriate similarity measure (referred to as a ‘kernel function’), $k : \mathcal{X} \times \mathcal{X} \rightarrow \mathbb{R}$, over a sample space, \mathcal{X} , any given probability distribution, P , over the same sample space can be embedded into a reproducing kernel Hilbert space via the mapping

$$P \mapsto \int_{x \in \mathcal{X}} k(x, \cdot) dP(x), \quad (5)$$

and for a large class of kernel functions this map is injective (Muandet et al., 2017). A number of independence tests and conditional independence tests have been developed

using the idea of embedding both the joint and product of marginal distributions of random variables, X and Y (possibly conditioned on a third variable Z for conditional independence tests), and estimating the distance between these embeddings (Gretton et al., 2008, 2005b; Jitkrittum et al., 2017; Zhang et al., 2012). For an injective embedding this distance is zero if and only if X and Y are independent; hence, a null hypothesis of independence can be rejected at a certain confidence if the estimated distance is sufficiently large. A permutation bootstrap can be used to approximate the sampling distribution of this estimated distance measure under the null. The Hilbert Schmidt Independence Criterion (HSIC) (Gretton et al., 2005a) is one such widely used measure which maps both distributions to Hilbert Schmidt operators between Hilbert spaces and estimates the Hilbert Schmidt norm between these operators.

We implemented a similar metric inspired by HSIC, the Finite Set Independence Criterion (FSIC), introduced by Jitkrittum et al. (2017), which we summarise here. Suppose we have random variables, $X \in \mathcal{X} \subset \mathbb{R}^n$ and $Y \in \mathcal{Y} \subset \mathbb{R}^m$, where \mathcal{X} , \mathcal{Y} are open sets, with marginal distributions, P_x and P_y , respectively and joint distribution, P_{xy} . Let $k : \mathcal{X} \times \mathcal{X} \rightarrow \mathbb{R}$ and $l : \mathcal{Y} \times \mathcal{Y} \rightarrow \mathbb{R}$ be positive definite kernel functions. Also let μ_x , μ_y and μ_{xy} be the embeddings of the distributions, P_x , P_y and P_{xy} , respectively, i.e.,

$$\mu_x = \int_{x \in \mathcal{X}} k(x, \cdot) dP_x(x) \quad (6)$$

$$\mu_y = \int_{y \in \mathcal{Y}} l(y, \cdot) dP_y(y) \quad (7)$$

$$\mu_{xy} = \int_{(x,y) \in \mathcal{X} \times \mathcal{Y}} k(x, \cdot) l(y, \cdot) dP_{xy}(x, y) \quad (8)$$

and define $\mu_x \mu_y(x, y) := \mu_x(x) \mu_y(y)$. Now $\mu_x \mu_y$ and μ_{xy} can be thought of as smooth functions and a distance measure between these functions is given by the mean squared distance between these functions evaluated at J random test locations. This defines the FSIC measure

$$\text{FSIC}^2 = \frac{1}{J} \sum_{i=1}^J [\mu_{xy}(v_i, w_i) - \mu_x(v_i) \mu_y(w_i)]^2$$

where $\{(v_i, w_i)\}_{i=1}^J$ are the randomly chosen test locations. Jitkrittum et al. (2017) derive a plug-in estimator for a normalised version of this criterion which can be computed in linear time and show under some assumptions that an independence test based on this normalised criterion is consistent. The assumption that \mathcal{X} and \mathcal{Y} are open sets restricts the use of FSIC to continuous variables. When discrete variables are present, more general measures could be used, such as HSIC, for which there exist approximations which also run in linear time (Zhang et al., 2018).

To construct conditional independence tests, we applied the *Regression with Subsequent Independence Test* method proposed by Peters et al. (2014). In this method, given random variables, X , Y and Z , a conditional independence test of X and Y given Z is performed by first applying a Gaussian process regression of X on Z and Y on Z and testing the residuals for independence, in our case using the FSIC as described above.

Flaxman et al. (2016) show that this produces a consistent conditional independence test.

2.3.3. *Spatiotemporal prewhitening*

In any spatiotemporal data there is likely to be spatiotemporal autocorrelation which presents two problems for learning causal relationships. Firstly, spatial or temporal structure can act as a confounder, inducing spurious associations between variables that could be misinterpreted as causal relationships (Flaxman et al., 2016). Secondly, observations cannot be treated as independent and identically distributed, a fundamental assumption in most, though not all (Zhang et al., 2009), independence tests, including the FSIC.

We follow the prewhitening procedure suggested by Flaxman et al. (2016) in which a geostatistical model is used to smooth each variable and remove spatiotemporal correlation from observations, returning approximately independent and identically distributed residuals which are then used as the inputs to the PC algorithm. We used Gaussian process regression with a separable Gaussian process defined by a Matérn spatial kernel in Kronecker product with linear exponential and circular exponential (Gneiting, 2013) kernels for the temporal innovations, the latter being designed to capture both seasonal and aseasonal trends.

2.3.4. *Causal selection procedure*

For each possible edge (equivalently for each possible directed causal relationship between any two variables), the output of the PC algorithm is binary, with this edge either present or not present, and therefore the algorithm does not provide a measure of certainty about the presence or absence of a given edge. The algorithm may also be sensitive to stochasticity in the hypothesis test procedure (due to the bootstrapping to obtain the null hypothesis distribution) if there exist variables that are not clearly (conditionally) dependent or independent of each other. This sensitivity will propagate through the algorithm, as the removal of any edge influences which independence relationships are tested in the following steps. To increase the stability of the algorithm and provide a measure of certainty for each edge in the output, we repeatedly sampled 1000 observations from the available training set and applied the above approach of prewhitening this data and then applying our two-step version of the PC algorithm. From the causal graphs produced, a variable was then selected if it was a parent of the malaria incidence in above a fixed proportion, $\lambda > 0$, of output graphs. The tuning parameter λ was chosen through cross-validation within the training dataset. The causal selection procedure was implemented in R and C++ using the Rcpp package (Eddelbuettel and Balamuta, 2017).

2.4. *LASSO selection*

Classical LASSO regularisation (Tibshirani, 1996) finds coefficients $\beta = (\beta_1, \dots, \beta_K)$ of a linear model that minimize squared error while subject to a constraint on the L_1 -norm

of this vector

$$\sum_{i=1}^K |\beta_i| < t, \quad (9)$$

equivalent to adding a term, $\lambda \sum_i |\beta_i|$, to the loss function to be minimised. Here λ and t are positive tuning parameters controlling the level of regularisation, with a larger λ or smaller t corresponding to stronger regularisation. The geometry of the L_1 -norm makes it more likely that small coefficient values will be shrunk to zero (compared to, for example, ridge regression which penalises the L_2 -norm of the coefficient values) which invites use of the LASSO as a tool for dichotomous variable selection.

In a Bayesian setting the Bayesian LASSO (Park and Casella, 2008) can be used, which places a Laplace prior with mean zero on each coefficient. The scale parameter of the Laplace prior corresponds to the tuning parameter λ in the classical LASSO, controlling the level of shrinkage. To use the LASSO for covariate selection, the model was fit using the Bayesian LASSO at varying levels of shrinkage and covariates were selected if the magnitude of their coefficients exceeded a fixed threshold. The optimal level of shrinkage and threshold value were chosen through cross validation within the training dataset.

3. Results

3.1. Linear model

The performance of the linear model under causal feature selection, LASSO feature selection, and no feature selection is shown with respect to overall correlation between the predicted and observed incidence rates in Fig. 3 and with respect to mean local correlation in Fig. 4. Each point represents an iteration of the model fit from a specific time point with a randomly selected training set of the specified size, and the correlations are in each instance computed only on members of the testing library (i.e., ‘genuine hold-outs’ from the fitting process). Recall from Section 2.2 that the overall correlation—the average correlation between predicted and observed values over all months and locations tested—is an indicator of model performance in the spatiotemporal interpolation of risk patterns, while the local correlation—the mean of correlations between observed and predicted time series at each location for the subsequent two years given a year of data—is an indicator of model performance in temporal forecasting of risk patterns. As there was no temporal component in the noise term in this model, the temporal structure was only informed by the covariates.

The overall correlation (spatiotemporal interpolation accuracy) between predicted and observed incidence rates was generally very similar for all selection methods. Compared to both no feature selection and LASSO feature selection, the correlation was often slightly higher when causal selection was used, but there were a small set of iterations for which using all features or LASSO feature sets was significantly better. These tended to be the iterations of the model fit to the first year of data (from January 2013) with different training set sizes, for which the causal feature sets were particularly small, containing only Rainfall at all time lags and vegetation at a three month lag. In contrast, LASSO selection focused on temperature suitability for *P. vivax* transmission for these

iterations, suggesting this variable aided prediction in the linear setting. Results for the mean local correlation (temporal forecasting) under the linear model more strongly favour causal feature selection, which performed much better than no feature selection in an overwhelming majority of instances, and much better than LASSO selection in a clear majority of instances.

Worth noting is that in the case of overall correlation (spatiotemporal interpolation accuracy) there was a clear improvement in performance of all models as the number of locations in the training set increased. This trend appears to be driven by the more accurate predictions for locations in the training set but does not reflect better predictions in the unobserved locations (testing set) as the relative size of the training set increased. We can see this in Figs 9 and 10 of the on-line supporting materials, where there is no clear relationship between training set size and overall correlation when restricted to only points in either the training set or the testing set (although the very lowest values were from the smallest training sets).

LASSO and causal selection generally selected very different feature sets (see Fig. 5), so similar overall correlation values suggest that the features had only a limited ability to inform the model's ability to predict spatial structure and most of this structure likely came from the spatially correlated noise component of the model. The predictive error of the model under different selection methods is shown in Fig. 11 of the supporting materials. This was not a metric used during either causal or LASSO selection but shows similar results to overall correlation, showing a small improvement in performance in the majority of cases under causal selection, compared to LASSO selection or no selection, but a small set of iterations for which causal selection performed worse.

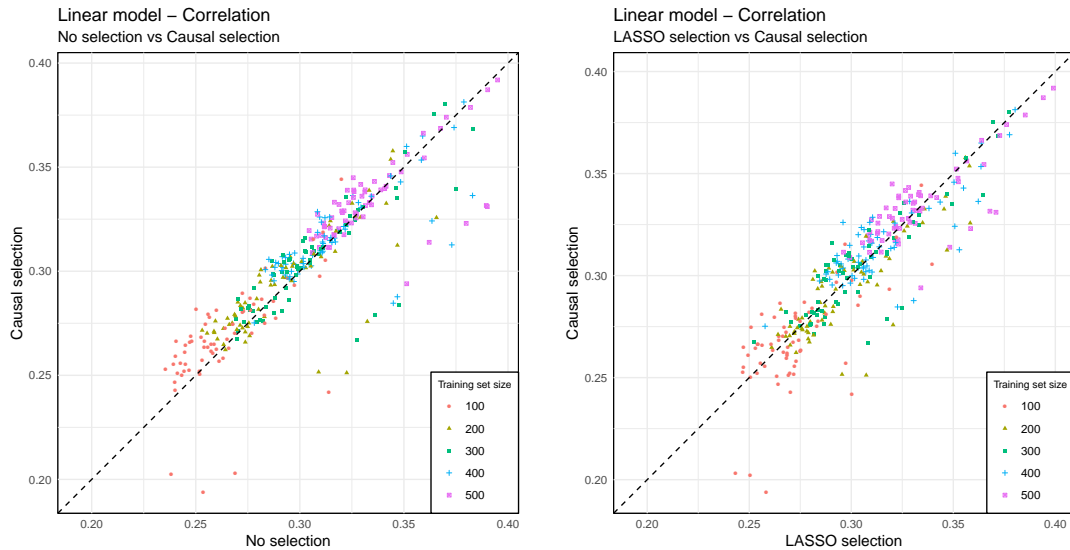


Fig. 3. Comparison of overall correlation between observed and predicted incidence rate from the linear model using causal selection and no selection (left) and LASSO selection (right).

The frequency of selection of each feature by causal and LASSO selection is shown in

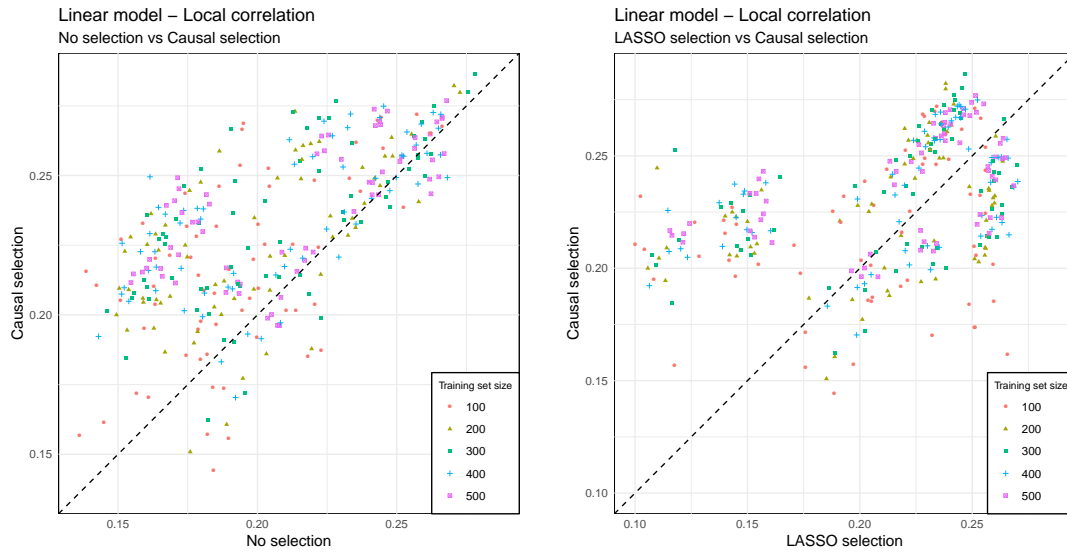


Fig. 4. Comparison of mean local correlations between observed and predicted incidence rate from the linear model using causal selection and no selection (left) and LASSO selection (right).

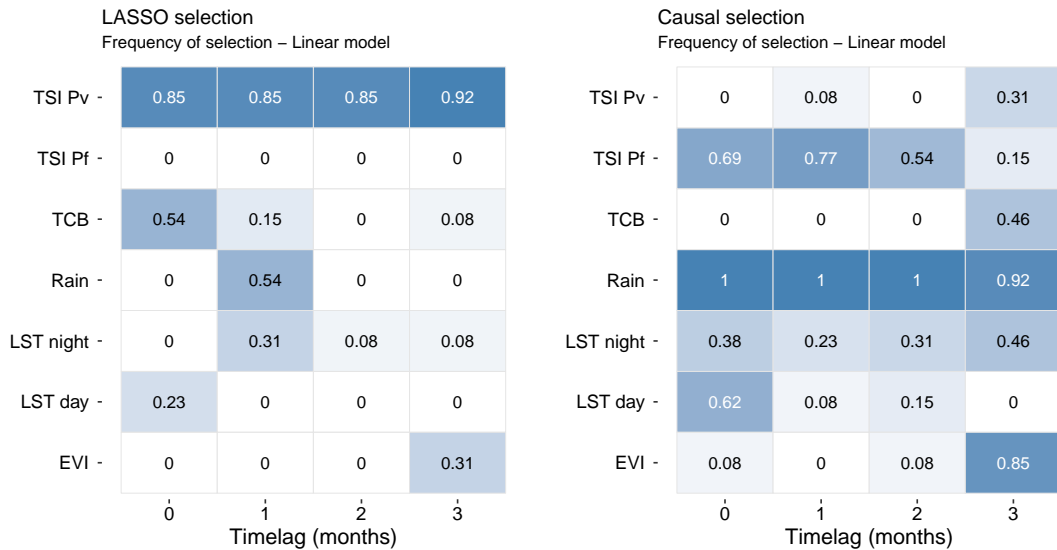


Fig. 5. Relative frequency of selection of each feature using LASSO selection (left) and causal selection (right) in the linear model.

Fig. 5. In general the causal feature sets were larger than those selected by LASSO, with an average size of 10.2 and 5.8 respectively. LASSO selection was also more consistent, selecting 13 distinct features across all iterations compared to 21 when causal selection

was used out of a total of 28. Causal selection placed a greater importance on rainfall, a biologically plausible cause of malaria risk, although it largely did not distinguish between rainfall at different time lags. LASSO selection only selected rainfall with a one month time lag but selected this feature less often than causal selection. Causal selection also placed importance on temperature suitability for *P. falciparum* transmission, with greatest importance at a one month lag, while LASSO selection generally selected temperature suitability for *P. vivax* transmission. Both of these species exist in Madagascar and it is likely that both selection methods had trouble distinguishing between these two similar variables. Temperature suitability for *P. vivax* may have had a more linear relationship with log-incidence and therefore have been selected by the LASSO, while temperature suitability for *P. falciparum* may have been preferred in the non-parametric causal selection as it is the dominant species in the country.

Fig. 6 shows the values of the coefficients for each feature across different iterations using no feature selection and (where selected) causal and LASSO selection. Across different iterations there was generally more variation in the size and sign of the coefficients for each feature when no feature selection was used. With causal and LASSO selection, there was generally more consistency in the sign of the coefficient for the features selected, although rainfall with two and three month time lags with causal selection was an exception to this. However, across the three methods there were generally similar coefficient values where the same features were selected. One exception to this is temperature suitability of *P. falciparum* at various time lags, which had a negative coefficient in many iterations when no selection was used but a positive coefficient with causal selection.

3.2. *Gaussian process model*

The performance of the GP model using causal selection and no selection is shown in Fig. 7. As with the linear model, there was little difference in the overall correlation between causal selection and no selection. However, unlike in the linear model, we do not observe iterations in which using all features was significantly better than the causal feature sets. This may be because the causal feature selection procedure, which was largely non-parametric, selected some covariates that had a non-linear relationship with incidence and therefore these feature sets performed worse in the linear model but comparably in the more flexible GP model.

The local correlation shows a similar pattern to the linear model, with causal selection usually performing better than using all features. Again, this suggests that using smaller causal feature sets improves the ability of the model to predict temporal patterns in risk. Fig. 8 shows the frequency of selection of each feature by the causal feature selection method. These were very similar to when causal feature selection was used in the linear model as the causal selection procedure is largely model-free, only using the model in the last step. As with the linear model, RMSE was not a metric that was used in the causal selection procedure but is shown in Fig. 16 of the supporting materials. In this model, the error is generally slightly higher when causal selection is used, with the greatest difference when the training set size is small where the error is high for both causal selection and no selection.

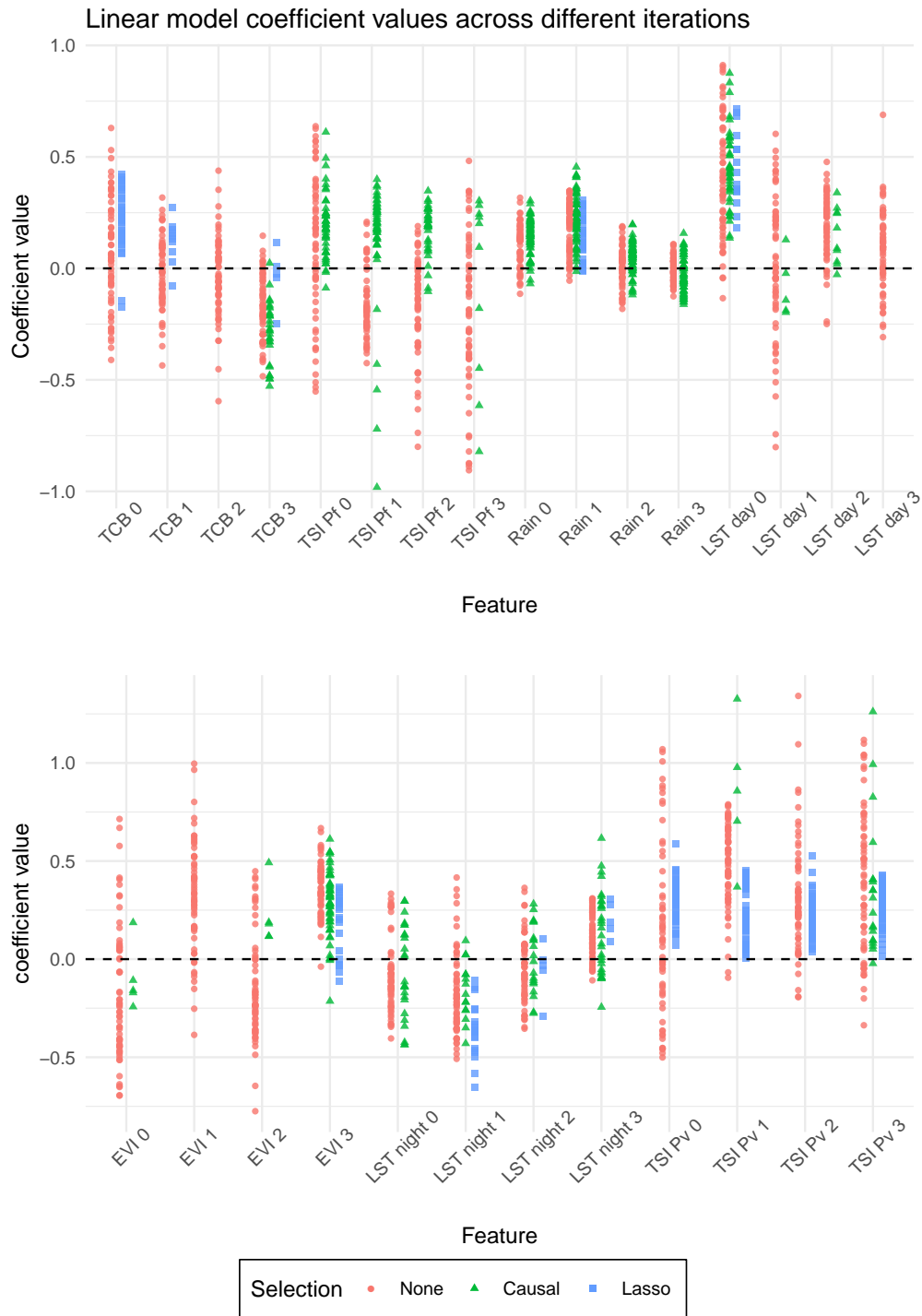


Fig. 6. Values of coefficients of different features in linear model across iterations for training sets of 500 locations.

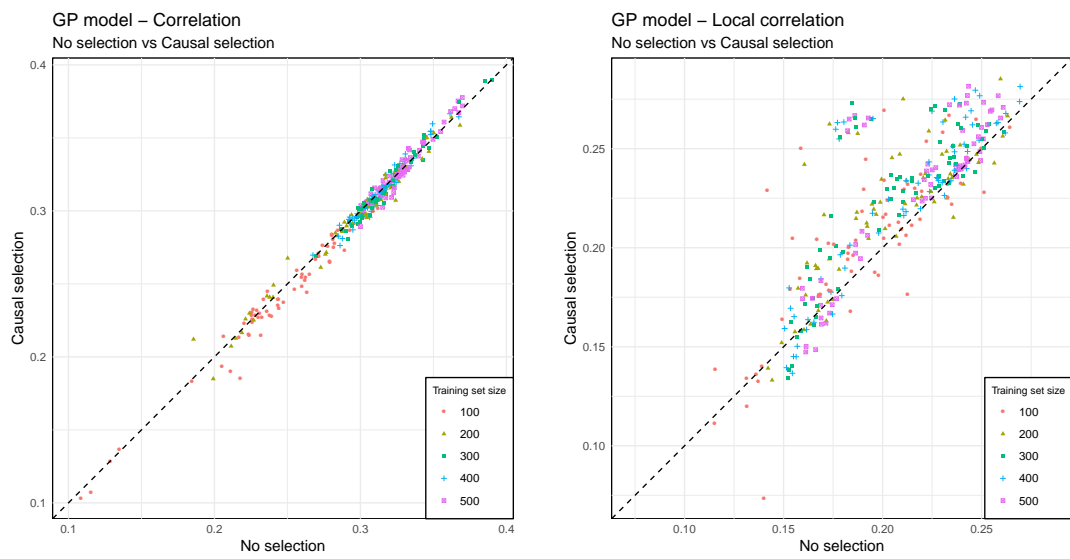


Fig. 7. Comparison of overall correlation (left) and local correlation (right) from the GP model using causal selection and no selection.

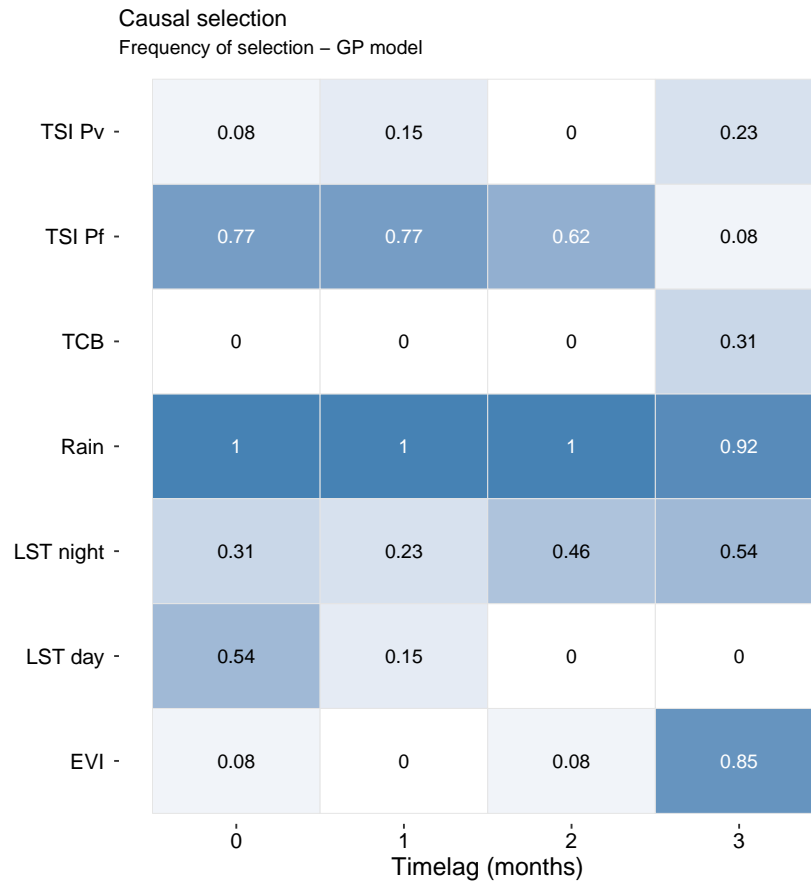


Fig. 8. Relative frequency of selection of each feature using causal selection (right) in the GP model.

4. Conclusion

We have shown that using the PC algorithm with non-parametric independence tests for causal feature selection is feasible for the kind of feature selection problems encountered in spatiotemporal disease mapping. The use of spatiotemporal prewhitening and kernel independence tests with linear complexity allow these methods to be applied to datasets with varied types of variables, spatiotemporal structure and large numbers of observations. In settings where the number of potential features is much greater than we have used here, applying the PC algorithm, which is exponential in complexity in the worst case, may not be possible. In these cases the general framework presented here could be used but with prewhitening and nonparametric tests used in combination with alternative causal discovery algorithms (Tsamardinos et al., 2003; Aliferis et al., 2003).

Within the Bayesian models we tested, causal feature selection showed similar performance to LASSO selection and no feature selection in terms of learning spatial patterns but improved performance for learning and predicting temporal patterns in malaria risk. The causal selection method we have used here is largely model-independent and could be made completely model-independent with an alternative method of choosing the tuning parameter λ , for example based on feature set size or background knowledge. This may be particularly useful for more complex, machine learning-style models where classical feature selection methods may not be suitable and where model evaluation (for example, to obtain cross-validation metrics for feature selection) may be expensive.

Although in this case causal feature selection did not uniformly outperform existing methods, there is also an appeal in having a fundamentally different approach of feature selection that performs comparably and can be used in combination with existing selection methods. For example, causal feature selection could be applied to investigate the robustness of existing methods.

Acknowledgements

Arsene Ratsimbaoa and Thierry Franchard of the National Malaria Control Program of Madagascar are thanked for sharing routine malaria case data with the Malaria Atlas Project. Fanjasoa Rakotomanana and her team at the Institut Pasteur de Madagascar are also thanked for sharing the health facility geolocation data with us. Suzanne Keddie and Emma Collins are thanked for processing the data.

The first author was supported in this work through an Engineering and Physical Sciences Research Council (EPSRC) (<https://epsrc.ukri.org/>) Systems Biology studentship award (EP/G03706X/1). Work by the Malaria Atlas Project on methods development for Malaria Eradication Metrics including this work is supported by a grant from the Bill and Melinda Gates Foundation (OPP1197730).

References

Ali, H., Cameron, E., Drovandi, C. C., McCaw, J. M., Guy, R. J., Middleton, M., El-Hayek, C., Hocking, J. S., Kaldor, J. M., Donovan, B. et al. (2015) A new approach to estimating trends in chlamydia incidence. *Sex Transm Infect*, **91**, 513–519.

- Aliferis, C. F., Tsamardinos, I. and Statnikov, A. (2003) HITON: a novel Markov Blanket algorithm for optimal variable selection. In *AMIA Annual Symposium Proceedings*, vol. 2003, 21. American Medical Informatics Association.
- Bhatt, S., Gething, P. W., Brady, O. J., Messina, J. P., Farlow, A. W., Moyes, C. L., Drake, J. M., Brownstein, J. S., Hoen, A. G., Sankoh, O. et al. (2013) The global distribution and burden of dengue. *Nature*, **496**, 504.
- Bhatt, S., Weiss, D., Cameron, E., Bisanzio, D., Mappin, B., Dalrymple, U., Battle, K., Moyes, C., Henry, A., Eckhoff, P. et al. (2015) The effect of malaria control on *Plasmodium falciparum* in Africa between 2000 and 2015. *Nature*, **526**, 207.
- Cawley, G. C. (2008) Causal & non-causal feature selection for ridge regression. In *Causation and Prediction Challenge*, 107–128.
- Chickering, D. M. (2002) Optimal structure identification with greedy search. *Journal of machine learning research*, **3**, 507–554.
- Colborn, K. L., Giorgi, E., Monaghan, A. J., Gudo, E., Candrinho, B., Marrufo, T. J. and Colborn, J. M. (2018) Spatio-temporal modelling of weekly malaria incidence in children under 5 for early epidemic detection in Mozambique. *Scientific reports*, **8**, 9238.
- Colombo, D. and Maathuis, M. H. (2014) Order-independent constraint-based causal structure learning. *The Journal of Machine Learning Research*, **15**, 3741–3782.
- Diggle, P. J., Moraga, P., Rowlingson, B. and Taylor, B. M. (2013) Spatial and spatio-temporal log-Gaussian Cox processes: extending the geostatistical paradigm. *Statistical Science*, **28**, 542–563.
- Drake, T. L., Lubell, Y., Kyaw, S. S., Devine, A., Kyaw, M. P., Day, N. P., Smithuis, F. M. and White, L. J. (2017) Geographic resource allocation based on cost effectiveness: an application to malaria policy. *Applied health economics and health policy*, **15**, 299–306.
- Eddelbuettel, D. and Balamuta, J. J. (2017) Extending extitR with extitC++: A Brief Introduction to extitRcpp. *PeerJ Preprints*, **5**, e3188v1. URL: <https://doi.org/10.7287/peerj.preprints.3188v1>.
- Elliot, P., Wakefield, J. C., Best, N. G. and Briggs, D. J. (2000) *Spatial epidemiology: methods and applications*. Oxford University Press.
- Flaxman, S. R., Neill, D. B. and Smola, A. J. (2016) Gaussian processes for independence tests with non-iid data in causal inference. *ACM Transactions on Intelligent Systems and Technology (TIST)*, **7**, 22.
- Funk, C. C., Peterson, P. J., Landsfeld, M. F., Pedreros, D. H., Verdin, J. P., Rowland, J. D., Romero, B. E., Husak, G. J., Michaelsen, J. C., Verdin, A. P. et al. (2014) A quasi-global precipitation time series for drought monitoring. *US Geological Survey Data Series*, **832**, 1–12.

- Gething, P. W., Casey, D. C., Weiss, D. J., Bisanzio, D., Bhatt, S., Cameron, E., Battle, K. E., Dalrymple, U., Rozier, J., Rao, P. C. et al. (2016) Mapping Plasmodium falciparum mortality in Africa between 1990 and 2015. *New England Journal of Medicine*, **375**, 2435–2445.
- Gething, P. W., Van Boeckel, T. P., Smith, D. L., Guerra, C. A., Patil, A. P., Snow, R. W. and Hay, S. I. (2011) Modelling the global constraints of temperature on transmission of Plasmodium falciparum and P. vivax. *Parasites & vectors*, **4**, 92.
- Girond, F., Randrianasolo, L., Randriamampionona, L., Rakotomanana, F., Randri-anarivelojosa, M., Ratsitorahina, M., Brou, T. Y., Herbreteau, V., Mangeas, M., Zigiumugabe, S. et al. (2017) Analysing trends and forecasting malaria epidemics in Madagascar using a sentinel surveillance network: a web-based application. *Malaria journal*, **16**, 72.
- Gneiting, T. (2013) Strictly and non-strictly positive definite functions on spheres. *Bernoulli*, **19**, 1327–1349.
- Gretton, A., Bousquet, O., Smola, A. and Schölkopf, B. (2005a) Measuring statistical dependence with Hilbert-Schmidt norms. In *International conference on algorithmic learning theory*, 63–77. Springer.
- Gretton, A., Fukumizu, K., Teo, C. H., Song, L., Schölkopf, B. and Smola, A. J. (2008) A kernel statistical test of independence. In *Advances in neural information processing systems*, 585–592.
- Gretton, A., Herbrich, R., Smola, A., Bousquet, O. and Schölkopf, B. (2005b) Kernel methods for measuring independence. *Journal of Machine Learning Research*, **6**, 2075–2129.
- Griffin, J. T., Bhatt, S., Sinka, M. E., Gething, P. W., Lynch, M., Patouillard, E., Shutes, E., Newman, R. D., Alonso, P., Cibulskis, R. E. et al. (2016) Potential for reduction of burden and local elimination of malaria by reducing Plasmodium falciparum malaria transmission: a mathematical modelling study. *The Lancet Infectious Diseases*, **16**, 465–472.
- Guyon, I., Aliferis, C. et al. (2007) Causal feature selection. In *Computational methods of feature selection*, 75–97. Chapman and Hall/CRC.
- Guyon, I. and Elisseeff, A. (2003) An introduction to variable and feature selection. *Journal of machine learning research*, **3**, 1157–1182.
- Haddawy, P., Hasan, A. I., Kasantikul, R., Lawpoolsri, S., Sa-angchai, P., Kaewkungwal, J. and Singhasivanon, P. (2018) Spatiotemporal Bayesian networks for malaria prediction. *Artificial intelligence in medicine*, **84**, 127–138.
- Hmamouche, Y., Casali, A. and Lakhal, L. (2017) A causality based feature selection approach for multivariate time series forecasting. In *DBKDA 2017, The Ninth International Conference on Advances in Databases, Knowledge, and Data Applications*.

- Howes, R. E., Franchard, T., Rakotomanga, T. A., Ramiranirina, B., Zikursh, M., Cramer, E. Y., Tisch, D. J., Kang, S. Y., Ramboarina, S., Ratsimbaoa, A. et al. (2018) Risk factors for malaria infection in central Madagascar: insights from a cross-sectional population survey. *The American journal of tropical medicine and hygiene*, **99**, 995–1002.
- Howes, R. E., Mioramalala, S. A., Ramiranirina, B., Franchard, T., Rakotorahalahy, A. J., Bisanzio, D., Gething, P. W., Zimmerman, P. A. and Ratsimbaoa, A. (2016) Contemporary epidemiological overview of malaria in Madagascar: operational utility of reported routine case data for malaria control planning. *Malaria journal*, **15**, 502.
- Jitkrittum, W., Szabó, Z. and Gretton, A. (2017) An adaptive test of independence with analytic kernel embeddings. In *Proceedings of the 34th International Conference on Machine Learning-Volume 70*, 1742–1751. JMLR. org.
- Kalisch, M. and Bühlmann, P. (2007) Estimating high-dimensional directed acyclic graphs with the PC-algorithm. *Journal of Machine Learning Research*, **8**, 613–636.
- Kang, S. Y., Battle, K. E., Gibson, H. S., Ratsimbaoa, A., Randrianariveojosia, M., Ramboarina, S., Zimmerman, P. A., Weiss, D. J., Cameron, E., Gething, P. W. et al. (2018) Spatio-temporal mapping of Madagascar’s Malaria Indicator Survey results to assess *Plasmodium falciparum* endemicity trends between 2011 and 2016. *BMC medicine*, **16**, 71.
- Kesteman, T., Rafalimanantsoa, S. A., Razafimandimby, H., Rasamimanana, H. H., Raharimanga, V., Ramarosandratana, B., Ratsimbaoa, A., Ratovonjato, J., Elissa, N., Randrianasolo, L. et al. (2016) Multiple causes of an unexpected malaria outbreak in a high-transmission area in Madagascar. *Malaria journal*, **15**, 57.
- Kesteman, T., Randrianariveojosia, M., Mattern, C., Raboanary, E., Pourette, D., Girond, F., Raharimanga, V., Randrianasolo, L., Piola, P. and Rogier, C. (2014) Nationwide evaluation of malaria infections, morbidity, mortality, and coverage of malaria control interventions in Madagascar. *Malaria journal*, **13**, 465.
- Kristensen, K., Nielsen, A., Berg, C. W., Skaug, H. and Bell, B. M. (2016) TMB: Automatic differentiation and Laplace approximation. *Journal of Statistical Software*, **70**, 1–21.
- Landier, J., Rebaudet, S., Piarroux, R. and Gaudart, J. (2018) Spatiotemporal analysis of malaria for new sustainable control strategies. *BMC medicine*, **16**, 226.
- Lawson, A., Biggeri, A., Böhning, D., Lesaffre, E., Viel, J.-F., Bertollini, R. et al. (1999) *Disease mapping and risk assessment for public health*. Wiley New York.
- Liu, H. and Motoda, H. (2007) *Computational methods of feature selection*. CRC Press.
- Minakawa, N., Sweijd, N., Behera, S. K., Hashizume, M., Ikeda, T., Kim, Y., Witbooi, P., Kruger, P., Landman, W., Maharaj, R. et al. (2018) Establishment of an early warning system for malaria in Southern Africa, incorporating climate predictions-overview of the iDEWS project. In *AGU Fall Meeting Abstracts*.

Muandet, K., Fukumizu, K., Sriperumbudur, B. and Schölkopf, B. (2017) Kernel mean embedding of distributions: A review and beyond. *Foundations and Trends in Machine Learning*, **10**, 1–141.

Nandy, P., Hauser, A. and Maathuis, M. H. (2018) High-dimensional consistency in score-based and hybrid structure learning. *The Annals of Statistics*, **46**, 3151–3183.

NASA Earth Data (2017a) Land processes distributed active archive center. https://lpdaac.usgs.gov/dataset_discovery/modis/modis_products_table/mcd43b5. [Accessed Sept 2017].

— (2017b) MODIS (MOD 13) - Gridded vegetation indices (NDVI and EVI). http://modis.gsfc.nasa.gov/data/dataproduct/dataproducts.php?MOD_NUMBER=13. [Accessed Sept 2017].

NASA Earth Observations (2017) Average land surface temperature. http://neo.gsfc.nasa.gov/view.php?datasetId=MOD_LSTD_CLIM_M. [Accessed Sept 2017].

Nguyen, M., Howes, R. E., Lucas, T. C., Battle, K. E., Cameron, E., Gibson, H. S., Rozier, J., Keddie, S., Collins, E., Arambepola, R. et al. (2019) A statistical modelling framework for mapping malaria seasonality. *arXiv preprint arXiv:1901.10782*.

Pan, W. K., Janko, M., Zaitchik, B. M., Feingold, B., Recalde, G. C., Mena, C., Pizzitutti, F. and Berky, A. (2018) Challenges for Malaria Early Warning Systems in the Amazon. In *AGU Fall Meeting Abstracts*.

Park, T. and Casella, G. (2008) The bayesian lasso. *Journal of the American Statistical Association*, **103**, 681–686.

Paszke, A., Gross, S., Massa, F., Lerer, A., Bradbury, J., Chanan, G., Killeen, T., Lin, Z., Gimelshein, N., Antiga, L., Desmaison, A., Kopf, A., Yang, E., DeVito, Z., Raison, M., Tejani, A., Chilamkurthy, S., Steiner, B., Fang, L., Bai, J. and Chintala, S. (2019) Pytorch: An imperative style, high-performance deep learning library. In *Advances in Neural Information Processing Systems 32* (eds. H. Wallach, H. Larochelle, A. Beygelzimer, F. d'Alché-Buc, E. Fox and R. Garnett), 8024–8035. Curran Associates, Inc. URL: <http://papers.neurips.cc/paper/9015-pytorch-an-imperative-style-high-performance-deep-learning-library.pdf>.

Pearl, J. (2009) Causal inference in statistics: An overview. *Statistics surveys*, **3**, 96–146.

Peters, J., Mooij, J. M., Janzing, D. and Schölkopf, B. (2014) Causal discovery with continuous additive noise models. *The Journal of Machine Learning Research*, **15**, 2009–2053.

R Core Team (2018) *R: A Language and Environment for Statistical Computing*. R Foundation for Statistical Computing, Vienna, Austria. URL: <https://www.R-project.org/>.

- Randrianasolo, L., Raelina, Y., Ratsitorahina, M., Ravolomanana, L., Andriamandimby, S., Heraud, J.-M., Rakotomanana, F., Ramanjato, R., Randrianarivo-Solofoniaina, A. E. and Richard, V. (2010) Sentinel surveillance system for early outbreak detection in Madagascar. *BMC Public Health*, **10**, 31.
- Reiner, R. C., Geary, M., Atkinson, P. M., Smith, D. L. and Gething, P. W. (2015) Seasonality of *Plasmodium falciparum* transmission: a systematic review. *Malaria journal*, **14**, 343.
- Ribeiro Jr, P. J., Diggle, P. J. et al. (2001) geoR: a package for geostatistical analysis. *R news*, **1**, 14–18.
- Rubin, D. B. (2005) Causal inference using potential outcomes: Design, modeling, decisions. *Journal of the American Statistical Association*, **100**, 322–331.
- Schölkopf, B., Janzing, D., Peters, J., Sgouritsa, E., Zhang, K. and Mooij, J. (2012) On causal and anticausal learning. *arXiv preprint arXiv:1206.6471*.
- Shearer, F. M., Huang, Z., Weiss, D. J., Wiebe, A., Gibson, H. S., Battle, K. E., Pigott, D. M., Brady, O. J., Putaporntip, C., Jongwutiwes, S. et al. (2016) Estimating geographical variation in the risk of zoonotic *Plasmodium knowlesi* infection in countries eliminating malaria. *PLoS neglected tropical diseases*, **10**, e0004915.
- Singh, N., Mishra, S., Singh, M. and Sharma, V. (2000) Seasonality of *Plasmodium vivax* and *P. falciparum* in tribal villages in central India (1987–1995). *Annals of Tropical Medicine & Parasitology*, **94**, 101–112.
- Spirtes, P., Glymour, C. N. and Scheines, R. (2000) *Causation, prediction, and search*. MIT press.
- Spirtes, P. and Meek, C. (1995) Learning Bayesian networks with discrete variables from data. In *KDD*, vol. 1, 294–299.
- Sun, Y., Li, J., Liu, J., Chow, C., Sun, B. and Wang, R. (2015) Using causal discovery for feature selection in multivariate numerical time series. *Machine Learning*, **101**, 377–395.
- Tibshirani, R. (1996) Regression shrinkage and selection via the lasso. *Journal of the Royal Statistical Society: Series B (Methodological)*, **58**, 267–288.
- Tompkins, A. M., Colón-González, F. J., Di Giuseppe, F. and Damanya, D. (2018) A dynamical climate-driven malaria early warning system evaluated in Uganda, Rwanda and Malawi. In *EGU General Assembly Conference Abstracts*, vol. 20, 15516.
- Tsamardinos, I., Aliferis, C. F., Statnikov, A. R. and Statnikov, E. (2003) Algorithms for large scale Markov Blanket discovery. In *FLAIRS conference*, vol. 2, 376–380.
- Tsamardinos, I., Brown, L. E. and Aliferis, C. F. (2006) The max-min hill-climbing Bayesian network structure learning algorithm. *Machine learning*, **65**, 31–78.
- Ushey, K., Allaire, J. and Tang, Y. (2019) *reticulate: Interface to 'Python'*. URL: <https://CRAN.R-project.org/package=reticulate>. R package version 1.13.

- Weiss, D. J., Bhatt, S., Mappin, B., Van Boeckel, T. P., Smith, D. L., Hay, S. I. and Gething, P. W. (2014) Air temperature suitability for *Plasmodium falciparum* malaria transmission in Africa 2000-2012: a high-resolution spatiotemporal prediction. *Malaria journal*, **13**, 171.
- Weiss, D. J., Nelson, A., Gibson, H., Temperley, W., Peedell, S., Lieber, A., Hancher, M., Poyart, E., Belchior, S., Fullman, N. et al. (2018) A global map of travel time to cities to assess inequalities in accessibility in 2015. *Nature*, **553**, 333.
- World Health Organization (2019) *World malaria report 2019*. World Health Organization.
- Zhang, K., Peters, J., Janzing, D. and Schölkopf, B. (2012) Kernel-based conditional independence test and application in causal discovery. *arXiv preprint arXiv:1202.3775*.
- Zhang, Q., Filippi, S., Gretton, A. and Sejdinovic, D. (2018) Large-scale kernel methods for independence testing. *Statistics and Computing*, **28**, 113–130.
- Zhang, X., Hu, Y., Xie, K., Wang, S., Ngai, E. and Liu, M. (2014) A causal feature selection algorithm for stock prediction modeling. *Neurocomputing*, **142**, 48–59.
- Zhang, X., Song, L., Gretton, A. and Smola, A. J. (2009) Kernel measures of independence for non-iid data. In *Advances in neural information processing systems*, 1937–1944.

A. Supporting material

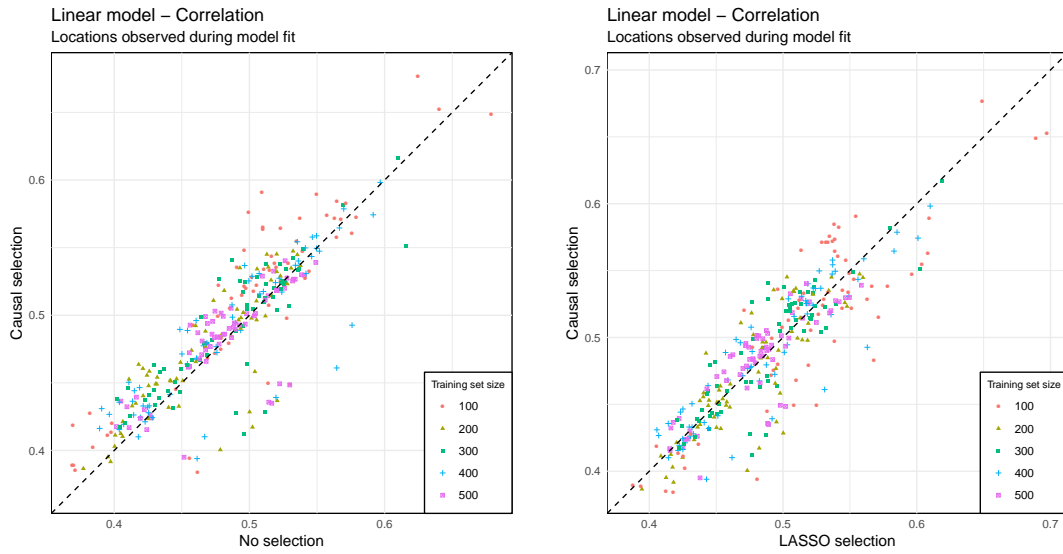


Fig. 9. Comparison of overall correlation from the linear model using causal selection and no selection (left) and LASSO selection (right) in locations observed during model fit.

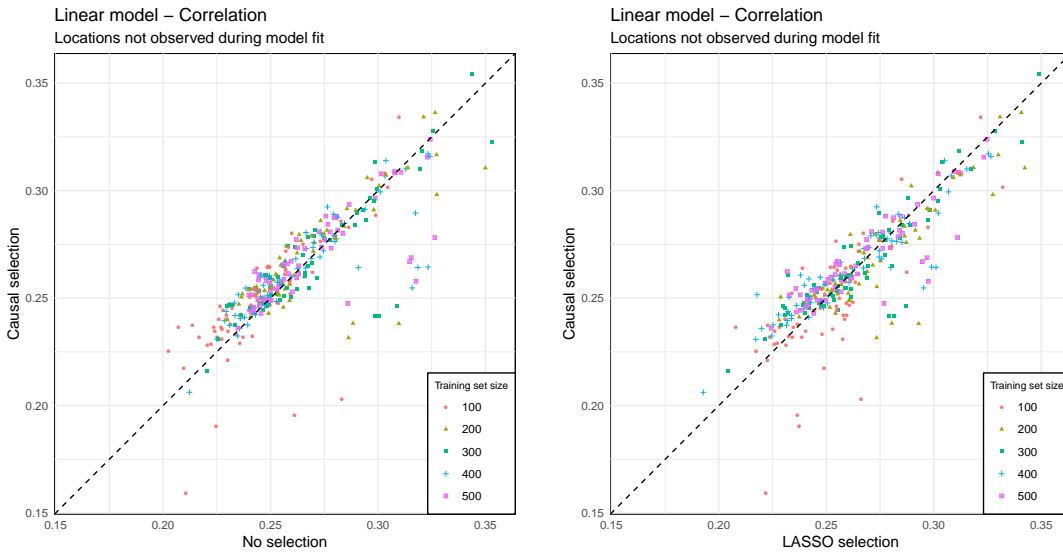


Fig. 10. Comparison of overall correlation from the linear model using causal selection and no selection (left) and LASSO selection (right) in locations not observed during model fit.

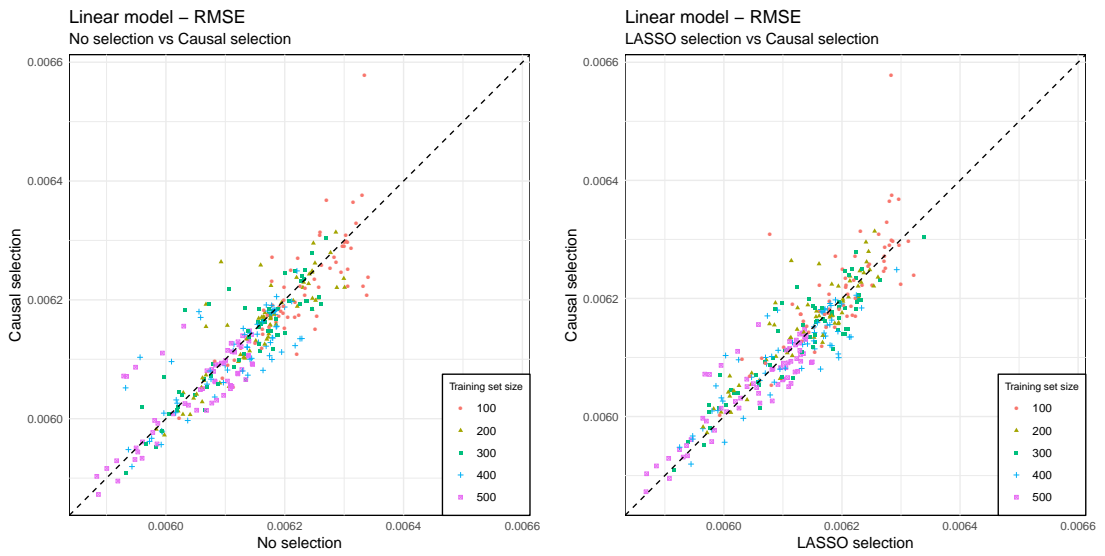


Fig. 11. Comparison of predictive error from the linear model using causal selection and no selection (left) and LASSO selection (right).

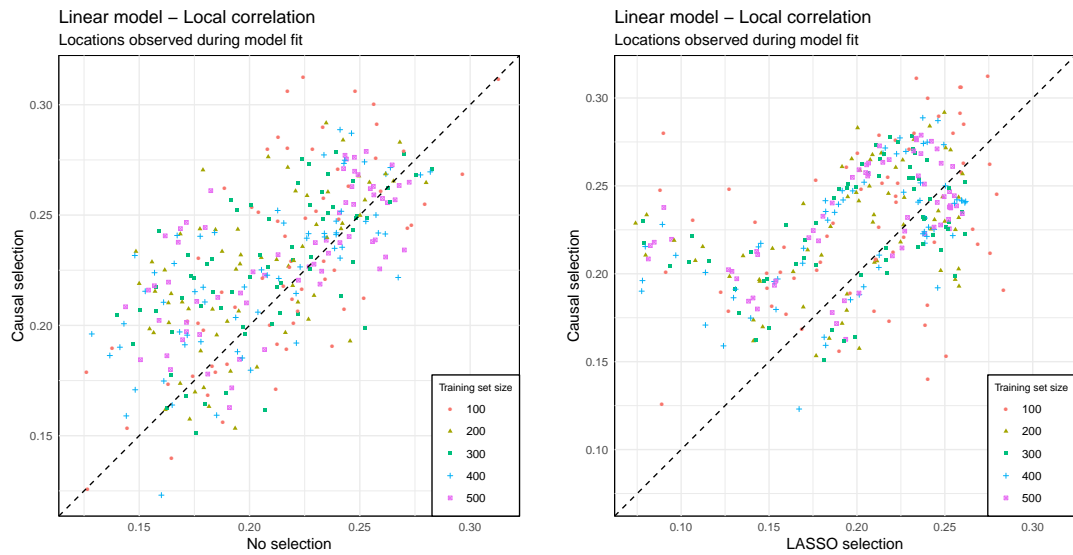


Fig. 12. Comparison of local correlation from the linear model using causal selection and no selection (left) and LASSO selection (right) in locations observed during model fit.

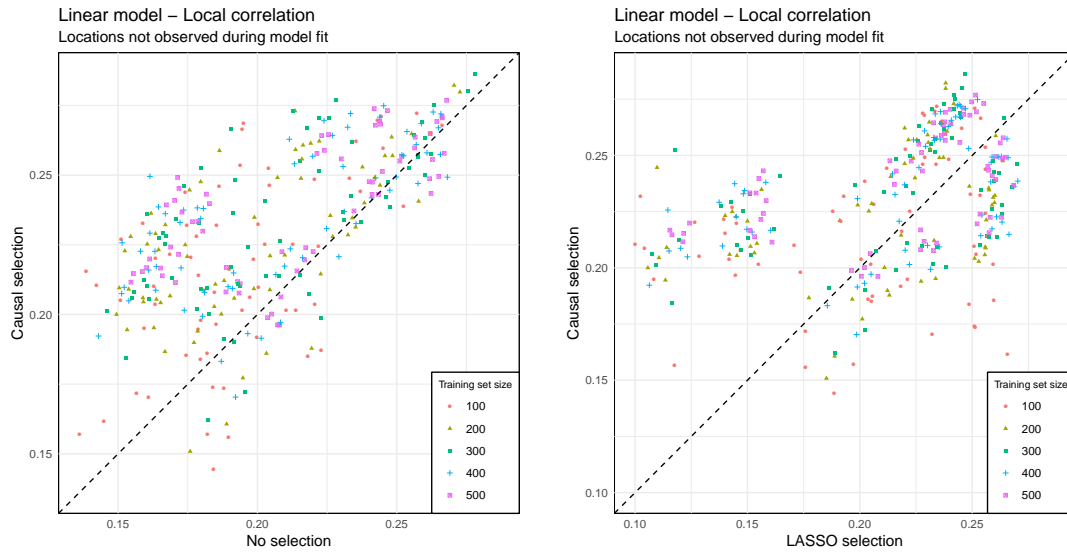


Fig. 13. Comparison of local correlation from the linear model using causal selection and no selection (left) and LASSO selection (right) in locations observed during model fit.

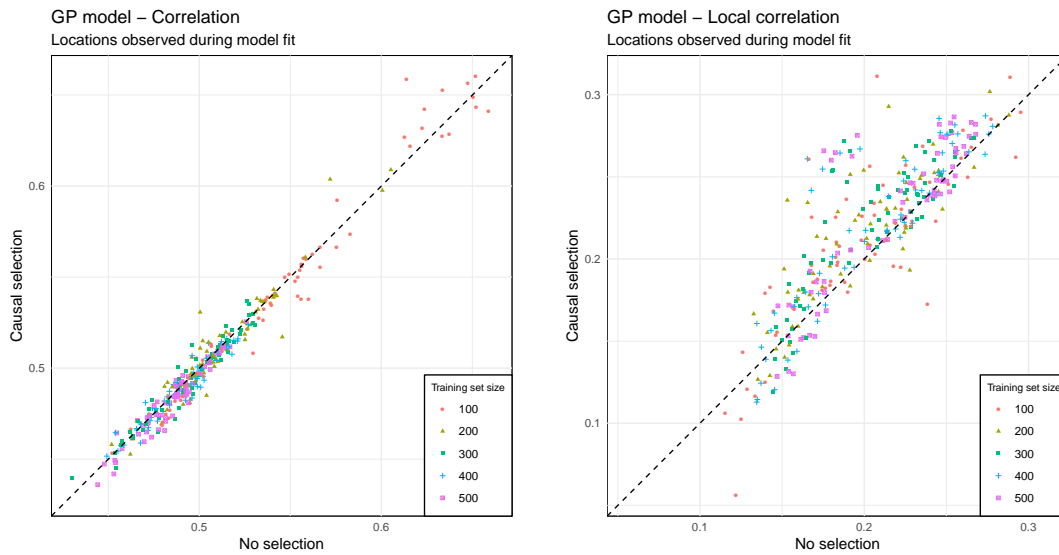


Fig. 14. Comparison of overall correlation (left) and local correlation (right) from the GP model using causal selection and no selection in locations observed during model fit.

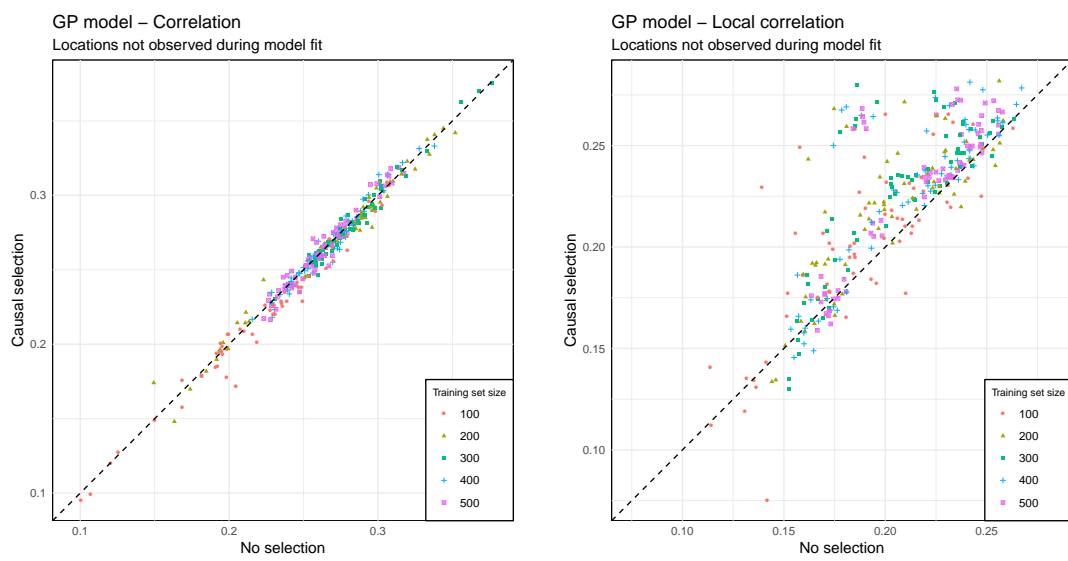


Fig. 15. Comparison of overall correlation (left) and local correlation (right) from the GP model using causal selection and no selection in locations not observed during model fit.

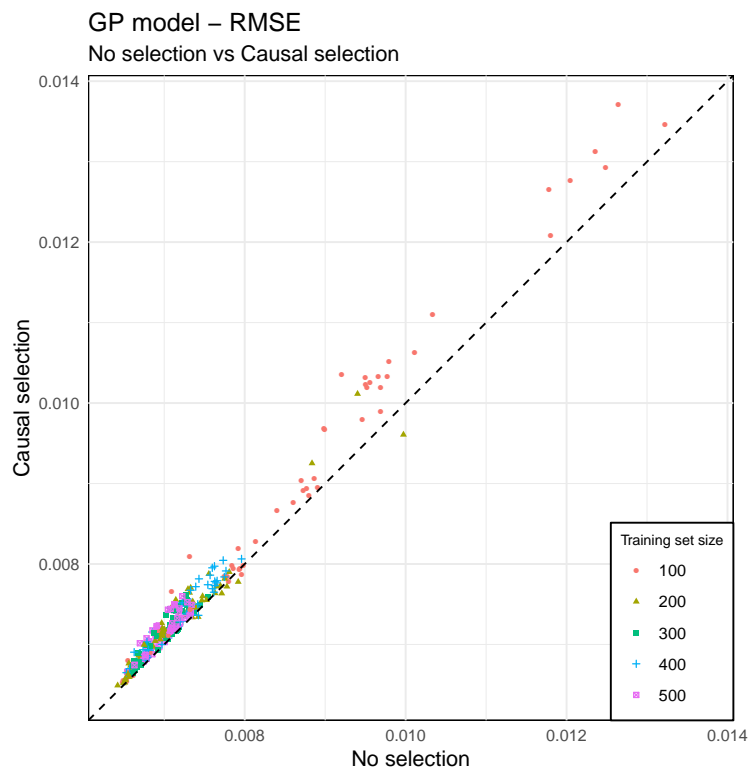


Fig. 16. Comparison of predictive error from the GP model using causal selection and no selection.

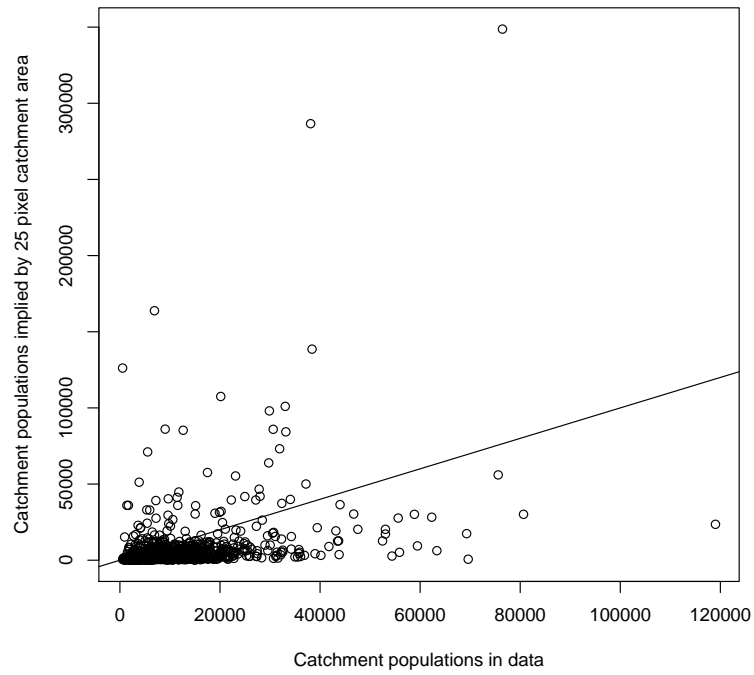


Fig. 17. Comparison of catchment populations from data and implied by a 25 km² catchment area. No correction has been made for overlapping areas which explains some of the high implied catchment populations, especially in population-dense regions where health facilities are closer together.